

Detailed quasiclassical dynamics of the $F^- + SiH_3Cl$ multi-channel reaction

Electronic Supplementary Information

Attila Á. Dékány and Gábor Czako*

MTA-SZTE Lendület Computational Reaction Dynamics Research Group, Interdisciplinary Excellence Centre
and Department of Physical Chemistry and Materials Science, Institute of Chemistry, University of Szeged,

Rerrich Béla tér 1, Szeged H-6720, Hungary

* E-mail: gczako@chem.u-szeged.hu

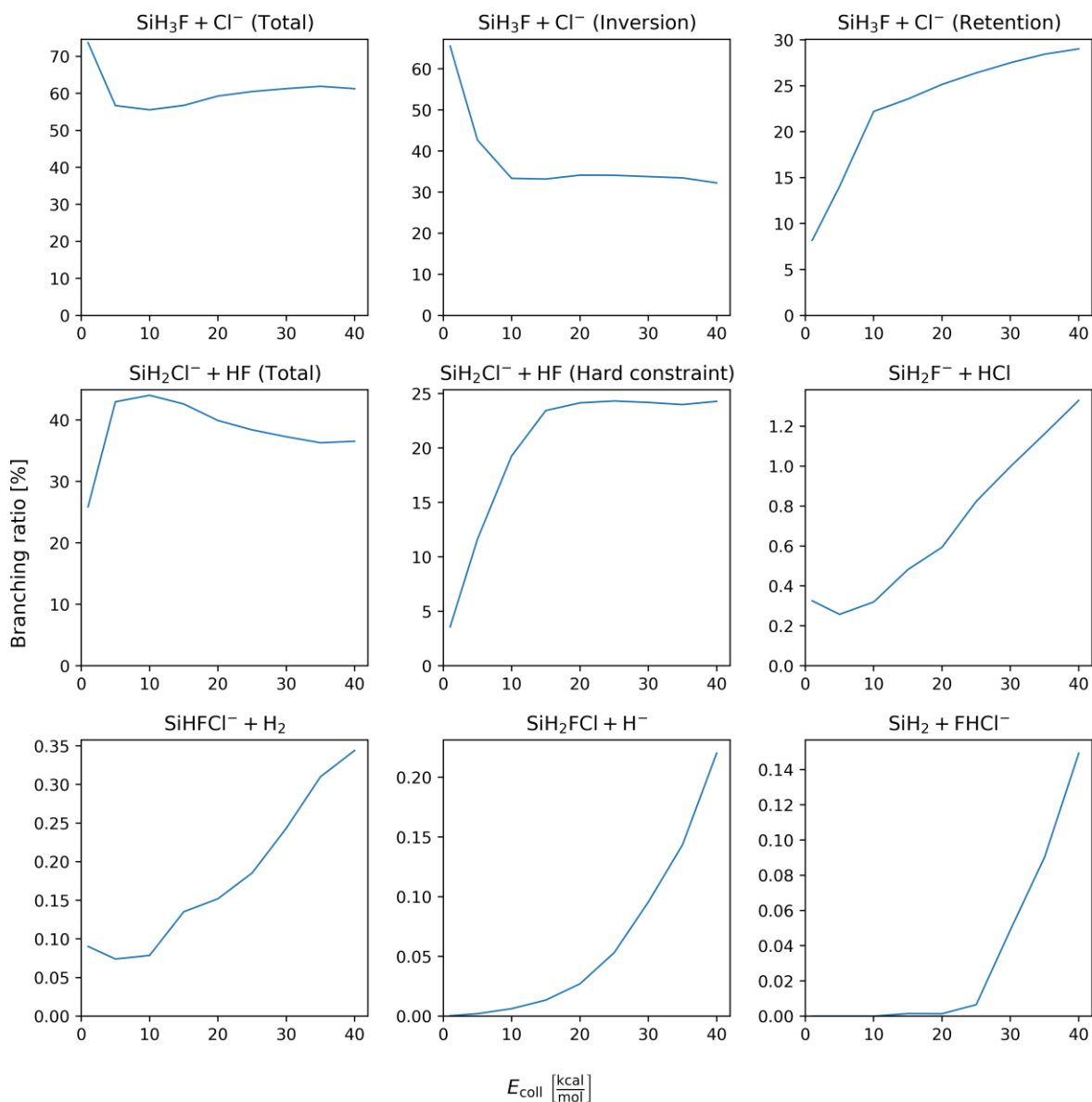


Figure S1. Branching ratios of the $\text{SiH}_3\text{Cl} + \text{F}^- \rightarrow \text{A} + \text{B}$ reactions as a function of collision energy. These ratios were calculated by dividing the cross section of the given product channel (with or without constraints) by the vibrationally-unconstrained total cross section.

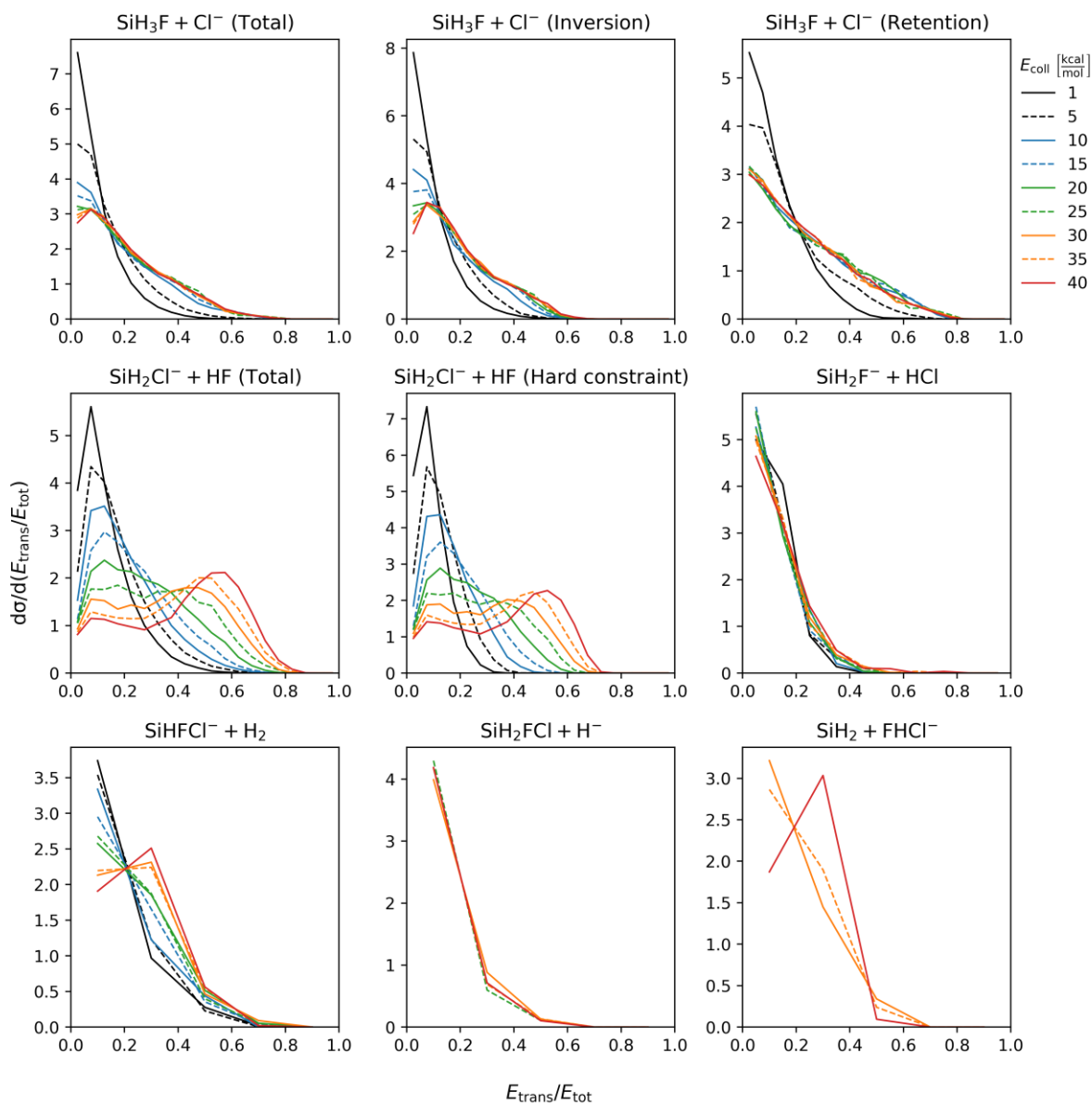


Figure S2. $E_{\text{trans}}/E_{\text{tot}}$ distributions of the $\text{SiH}_3\text{Cl} + \text{F}^- \rightarrow \text{A} + \text{B}$ reactions as a function of collision energy.

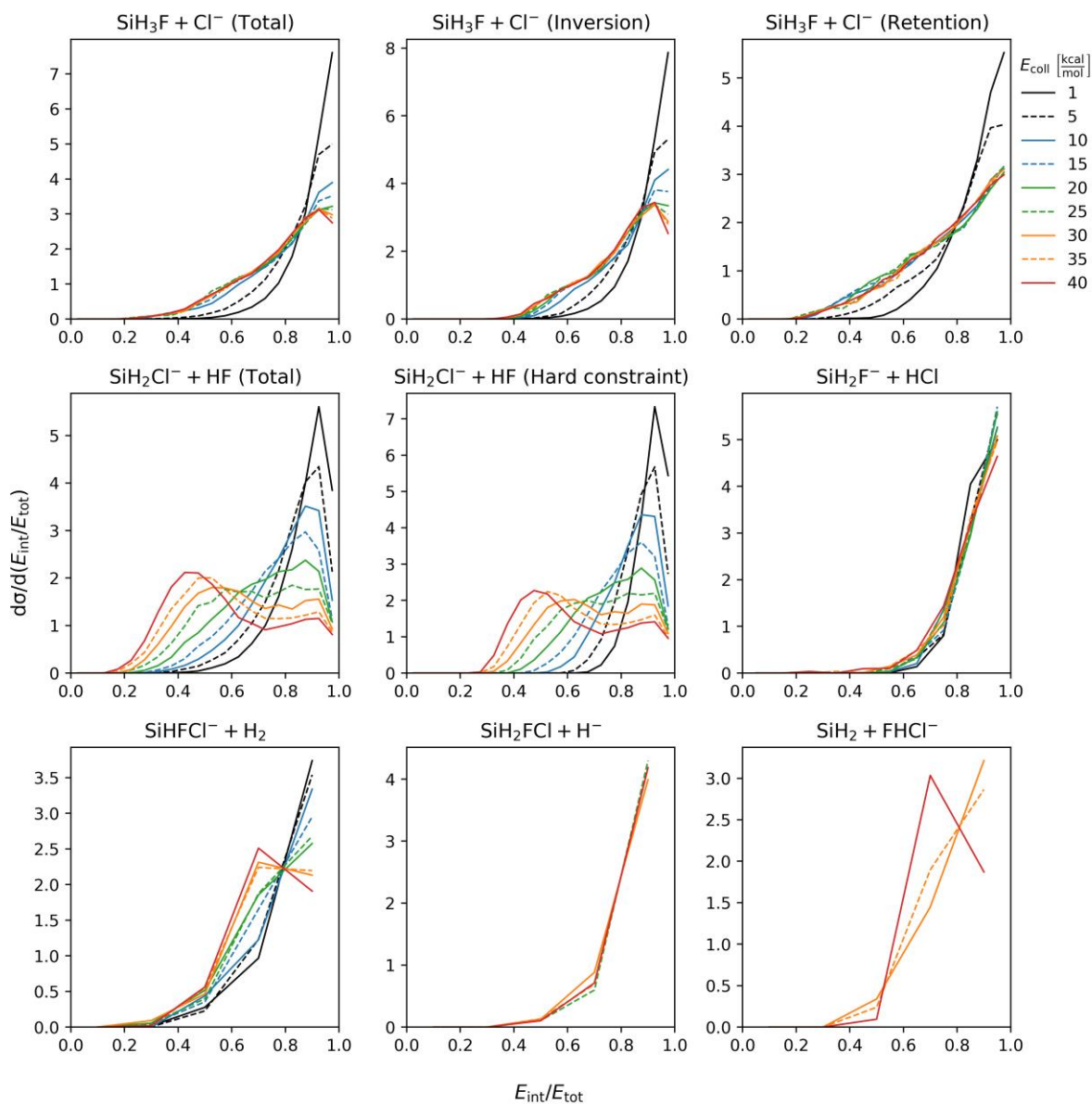


Figure S3. $E_{\text{int}}/E_{\text{tot}}$ distributions of the $\text{SiH}_3\text{Cl} + \text{F}^- \rightarrow \text{A} + \text{B}$ reactions as a function of collision energy.

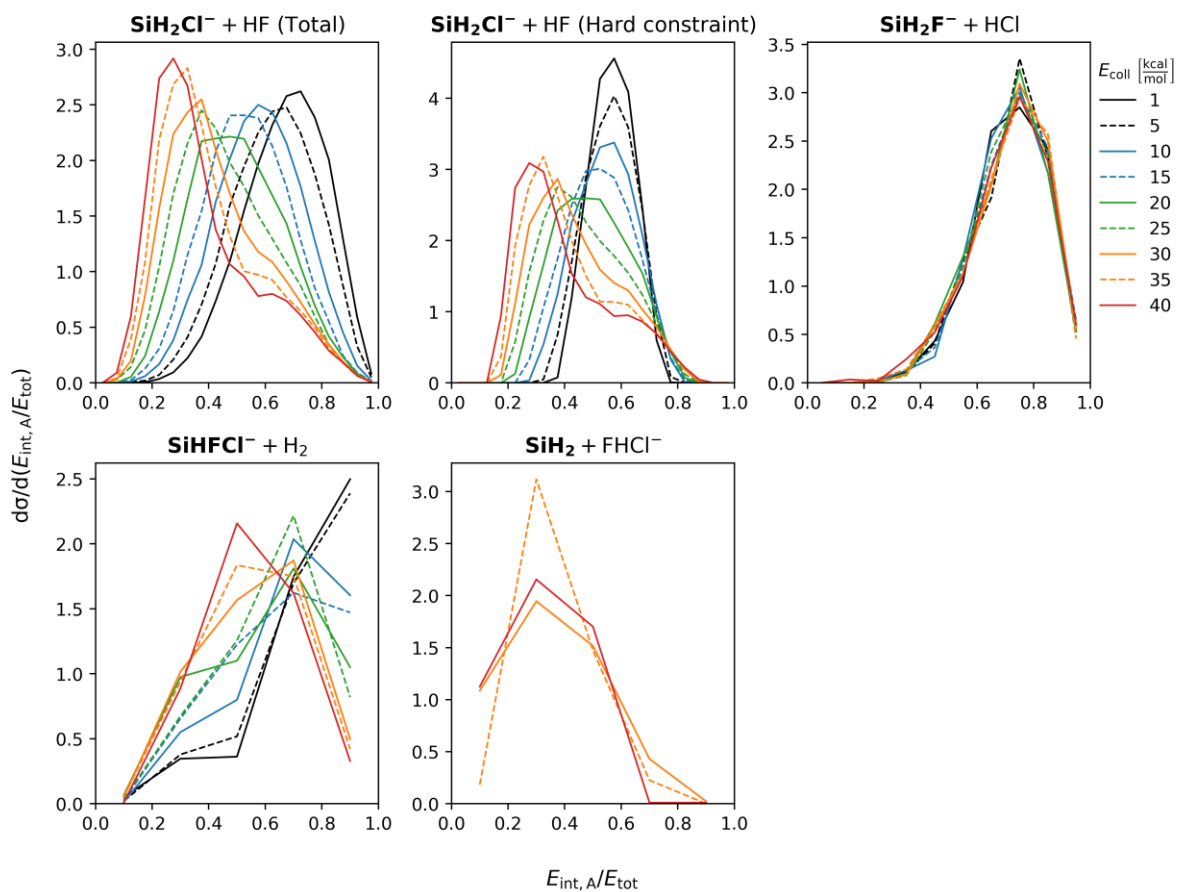


Figure S4. $E_{int,A}/E_{tot}$ distributions of the $\text{SiH}_3\text{Cl} + \text{F}^- \rightarrow \text{A} + \text{B}$ reactions as a function of collision energy where both A and B are polyatomic.

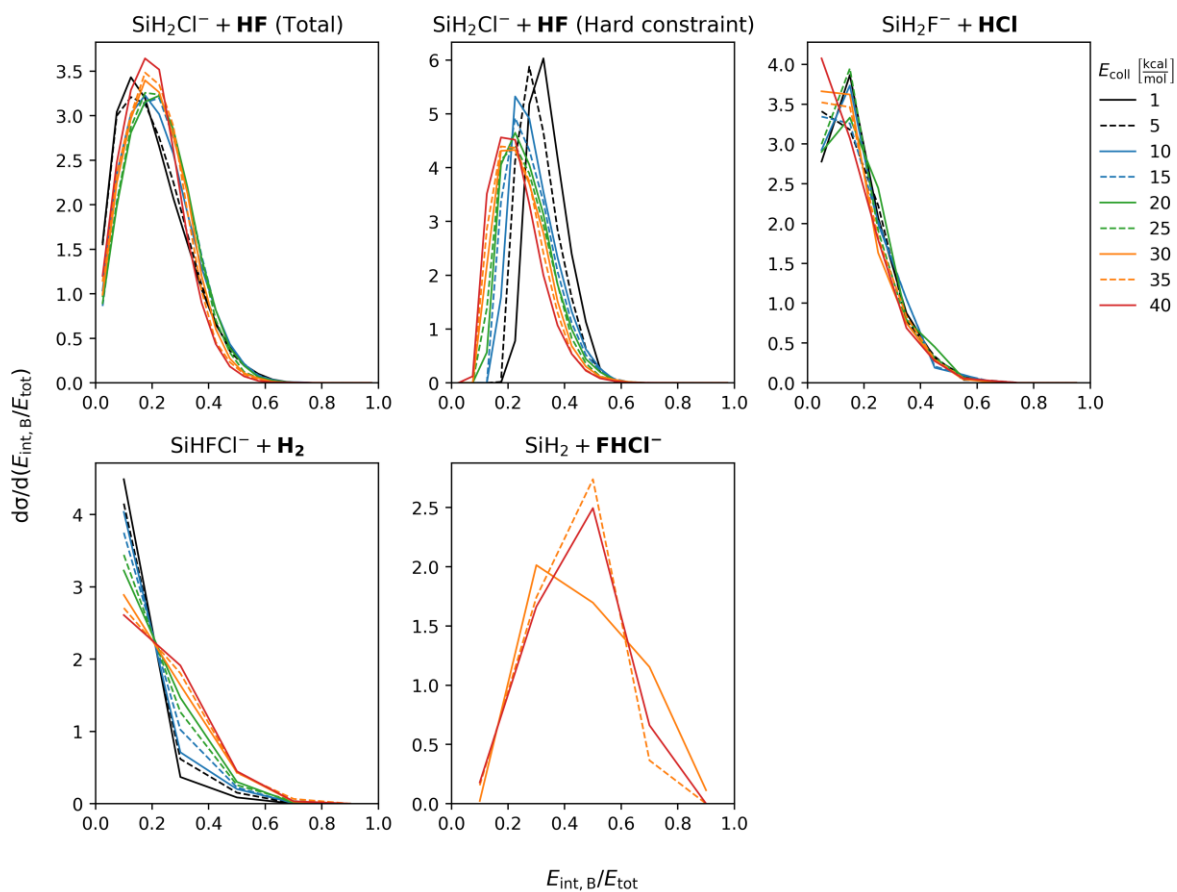


Figure S5. $E_{int,B}/E_{tot}$ distributions of the $\text{SiH}_3\text{Cl} + \text{F}^- \rightarrow \text{A} + \text{B}$ reactions as a function of collision energy where both A and B are polyatomic.

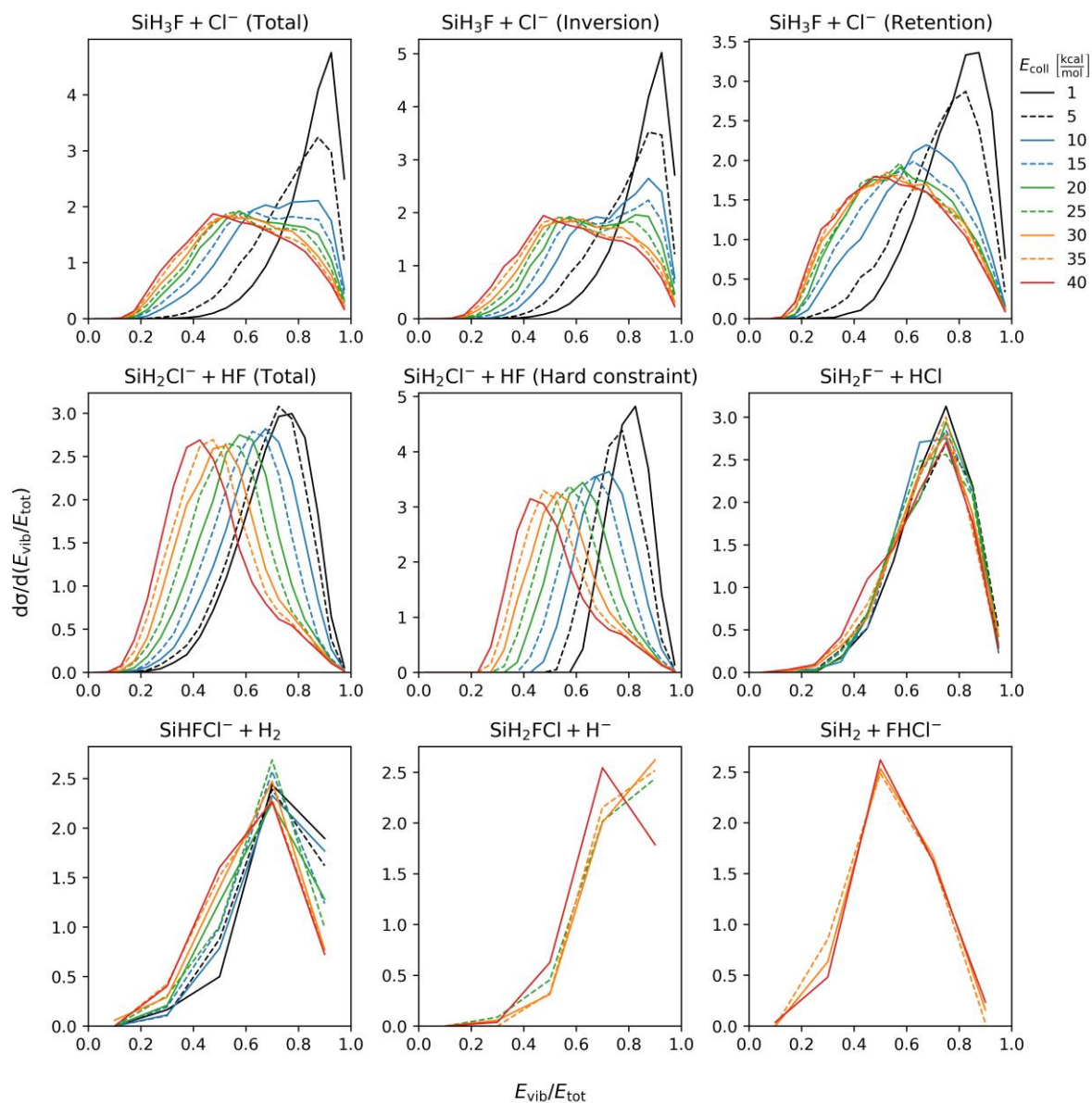


Figure S6. $E_{\text{vib}}/E_{\text{tot}}$ distributions of the $\text{SiH}_3\text{Cl} + \text{F}^- \rightarrow \text{A} + \text{B}$ reactions as a function of collision energy.

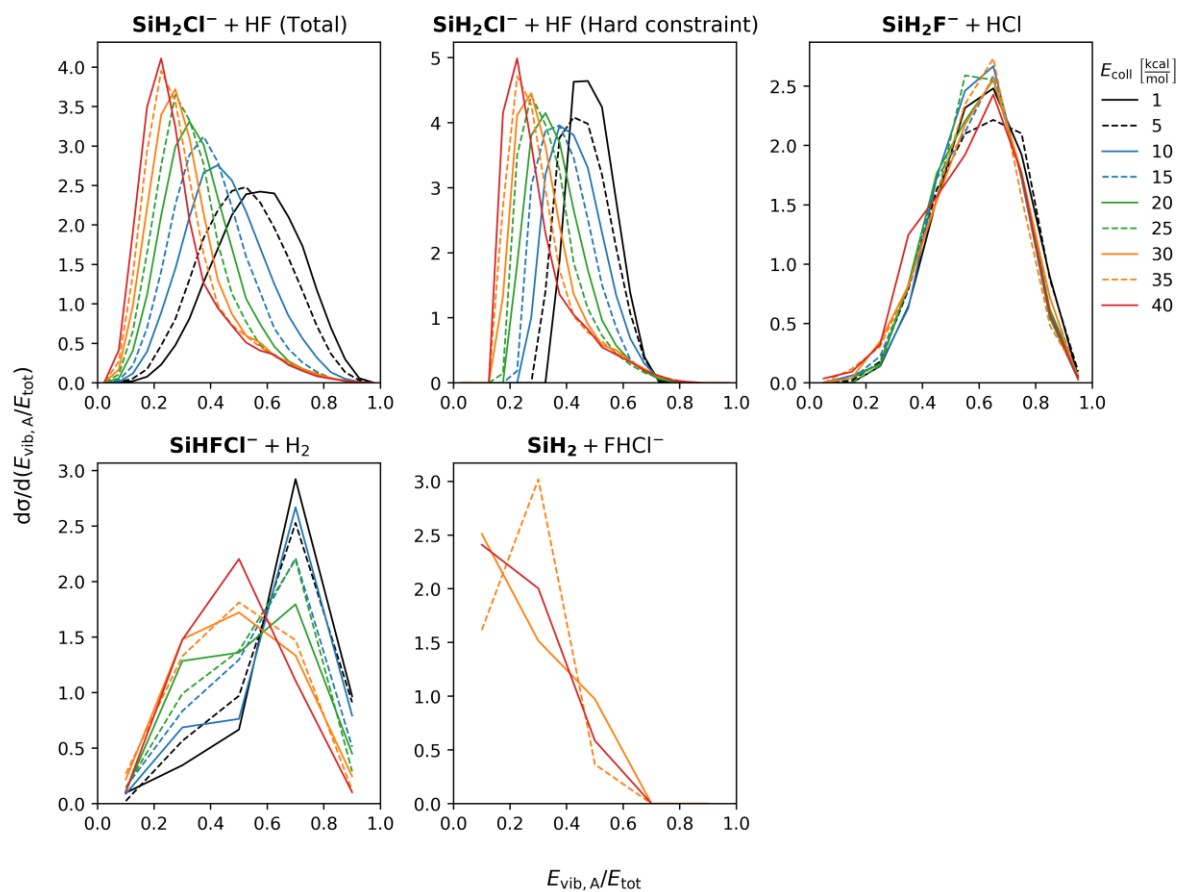


Figure S7. $E_{\text{vib},A}/E_{\text{tot}}$ distributions of the $\text{SiH}_3\text{Cl} + \text{F}^- \rightarrow \text{A} + \text{B}$ reactions as a function of collision energy where both A and B are polyatomic.

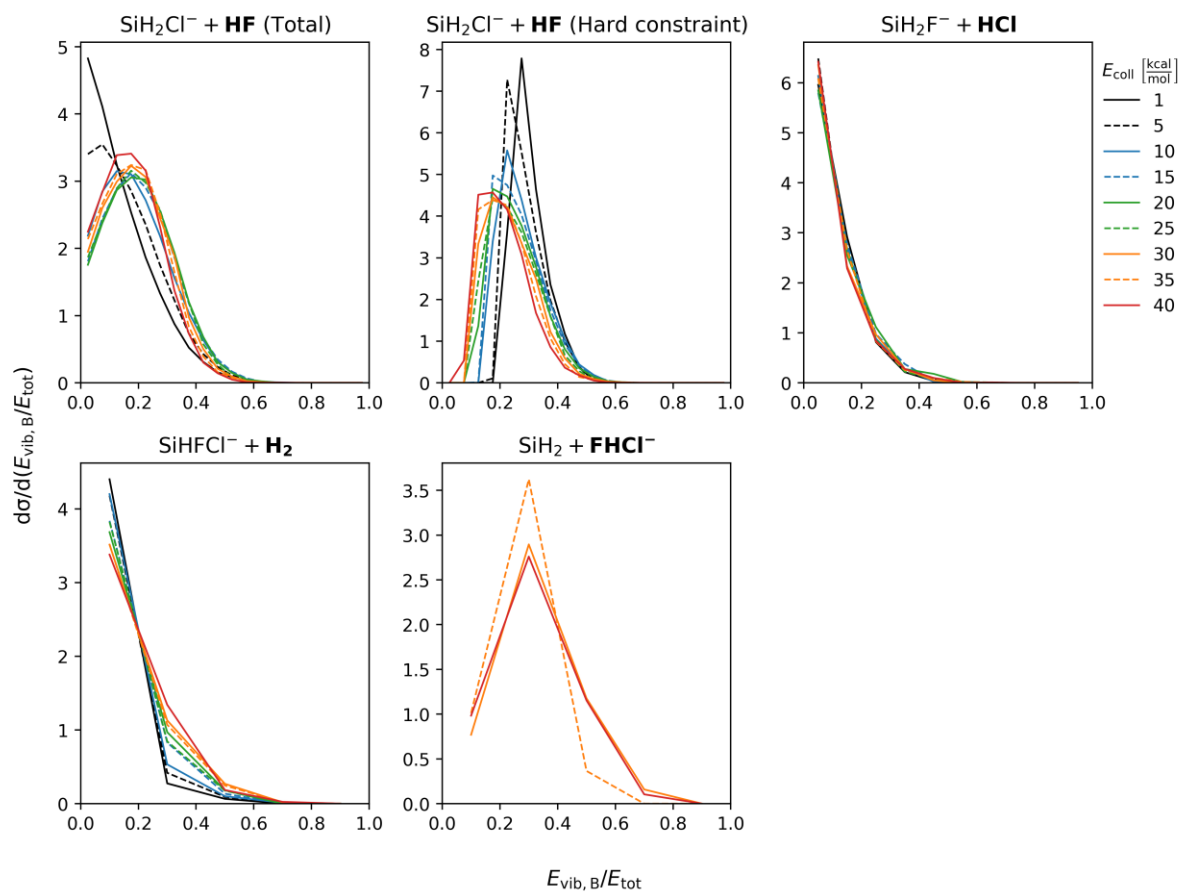


Figure S8. $E_{\text{vib},B}/E_{\text{tot}}$ distributions of the $\text{SiH}_3\text{Cl} + \text{F}^- \rightarrow \text{A} + \text{B}$ reactions as a function of collision energy where both A and B are polyatomic.

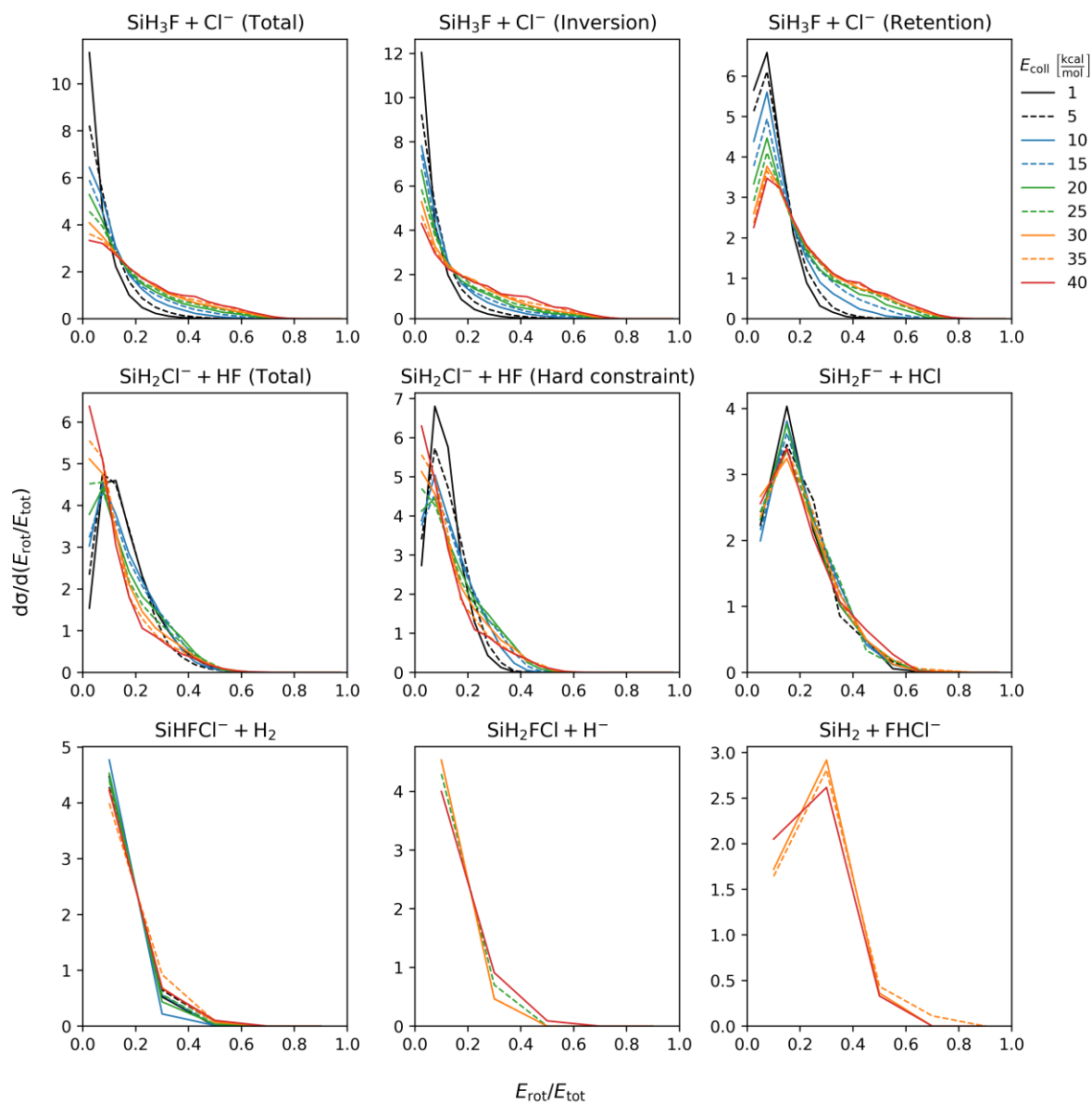


Figure S9. $E_{\text{rot}}/E_{\text{tot}}$ distributions of the $\text{SiH}_3\text{Cl} + \text{F}^- \rightarrow \text{A} + \text{B}$ reactions as a function of collision energy.

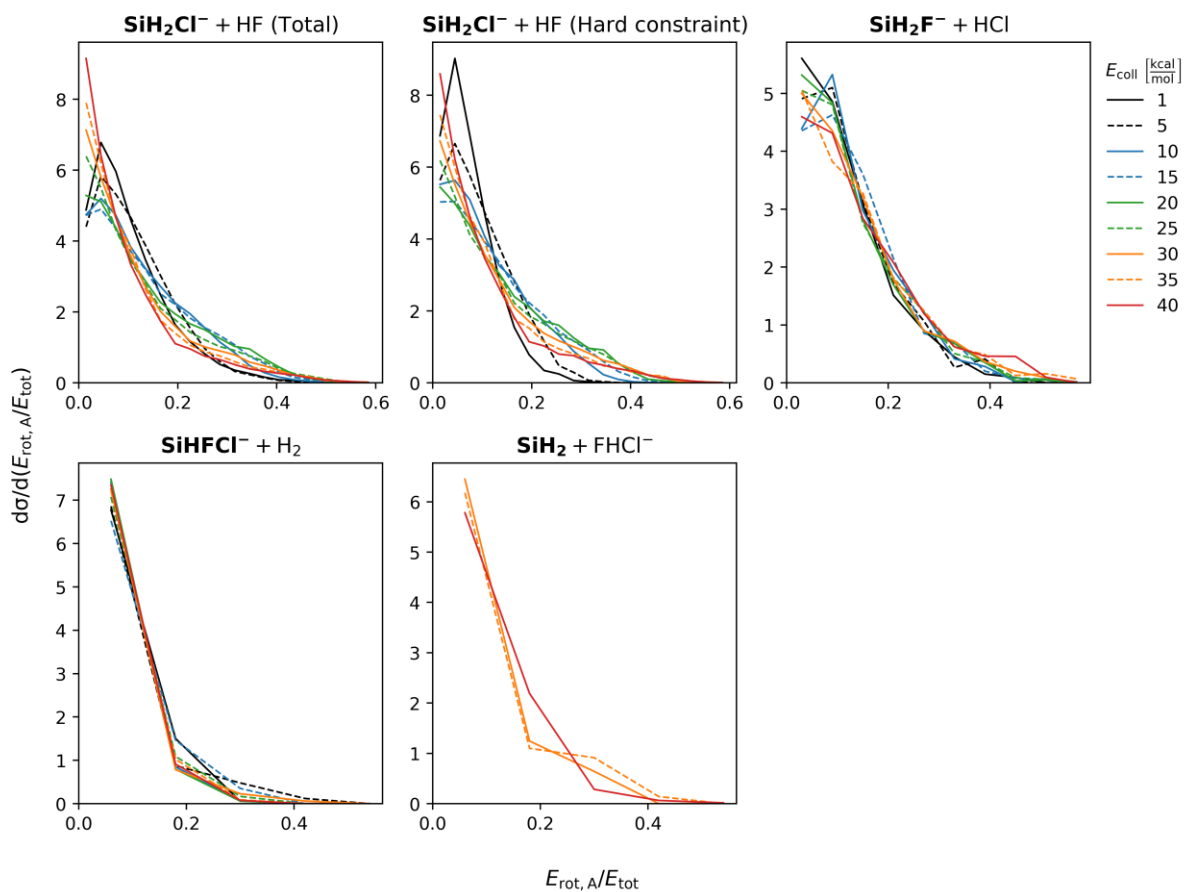


Figure S10. $E_{rot,A}/E_{tot}$ distributions of the $\text{SiH}_3\text{Cl} + \text{F}^- \rightarrow \text{A} + \text{B}$ reactions as a function of collision energy where both A and B are polyatomic.

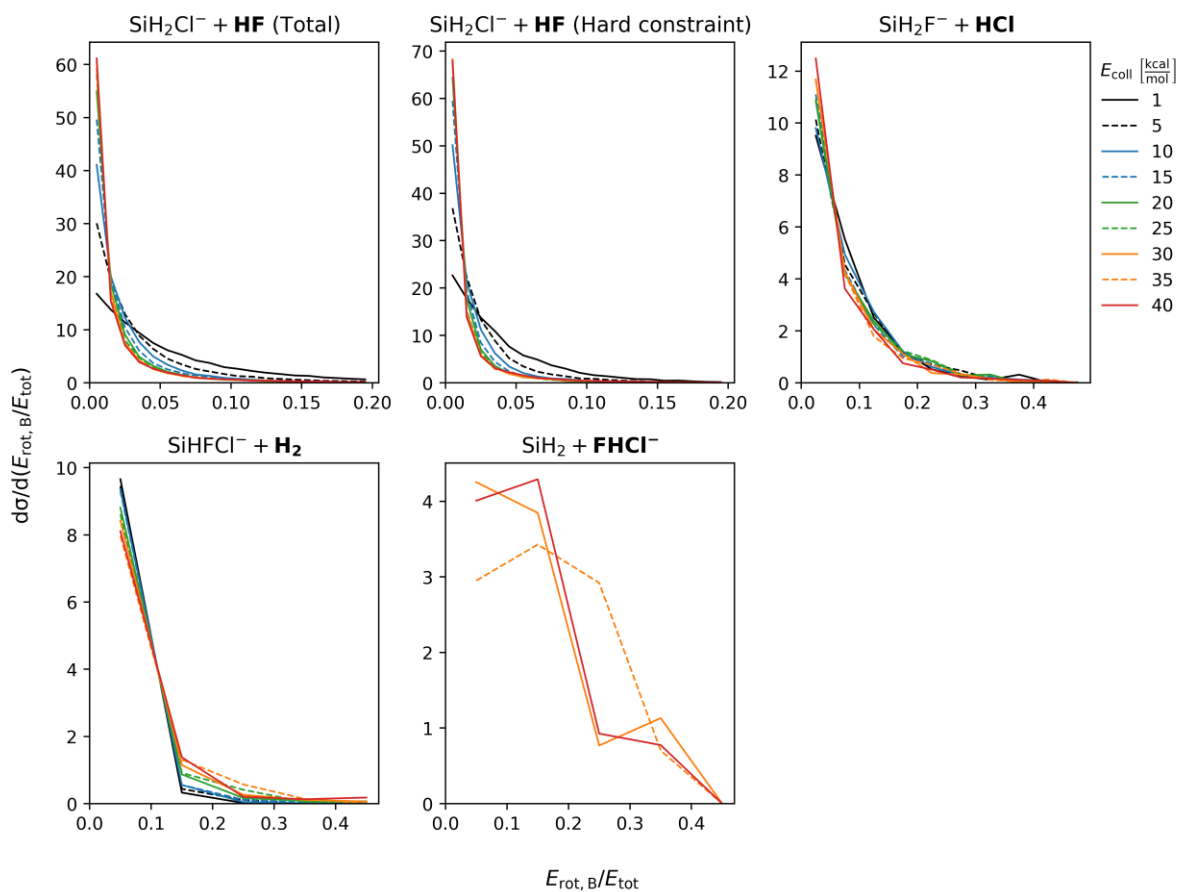


Figure S11. $E_{rot,B}/E_{tot}$ distributions of the $\text{SiH}_3\text{Cl} + \text{F}^- \rightarrow \text{A} + \text{B}$ reactions as a function of collision energy where both A and B are polyatomic.

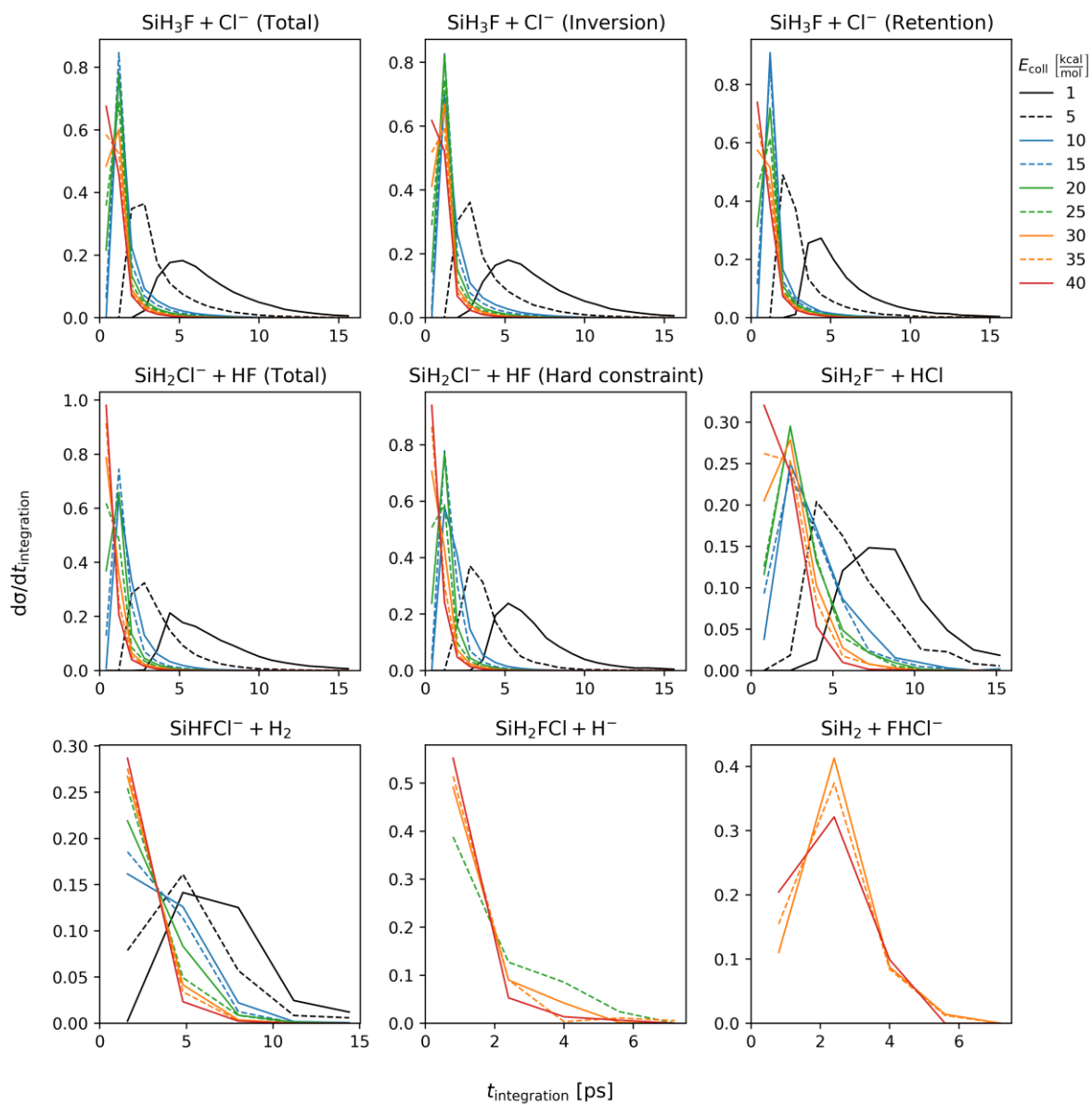


Figure S12. Integration time distributions of the $\text{SiH}_3\text{Cl} + \text{F}^- \rightarrow \text{A} + \text{B}$ reactions as a function of collision energy.